Magnetic polaron in ferro- and antiferromagnetic semiconductors

W. Nolting, S. Mathi Jaya, and S. Rex
Humboldt-Universität zu Berlin, Institut für Physik, Lehrstuhl Festkörpertheorie, Invalidenstrasse 110, 10115 Berlin, Germany
(Received 19 March 1996; revised manuscript received 28 June 1996)

The temperature-dependent quasiparticle spectrum of a single conduction electron exchange coupled to a ferro- or antiferromagnetically ordered localized-spin system (e.g., EuO, EuTe) is calculated by a moment-conserving Green function technique. In the weak coupling regime the exchange interaction leads to an almost rigid shift of the Bloch dispersion. The induced spin splitting of the conduction band states is proportional to the magnetization $\langle S^z \rangle$ of the localized-spin system. As soon as the coupling constant exceeds a critical value an additional splitting of the quasiparticle dispersion for each spin projection sets in due to different elementary excitations. One is based on a repeated emission and reabsorption of a magnon by the conduction electron resulting in an effective attraction between magnon and electron. This gives rise to a polaronlike quasiparticle (''magnetic polaron''). Another excitation is due to a direct magnon emission or absorption by the electron thereby flipping its own spin (''scattering states''). For the exactly calculable special case of a ferromagnetically saturated spin system ($T=0$ K), the magnetic polaron appears only in the $\downarrow$ spectrum and turns out to be a stable quasiparticle. For finite temperatures it gets a finite lifetime. In antiferromagnetic systems each quasiparticle band exhibits an additional ''Slater splitting'' due to the reduced magnetic Brillouin zone. The predicted strong correlation effects in the excitation spectrum require unconventional interpretations of respective inverse photoemission experiments. [S0163-1829(96)01344-6]

I. INTRODUCTION

The intensively investigated s-f model[1–3] describes the exchange coupling of itinerant electrons to localized magnetic moments. Such a situation is found in magnetic semiconductors like the europium chalcogenides[4] EuX(X=O, S, Se, Te) and the chromium chalcogenide spinels[5] $M\mathrm{Cr}_2\mathrm{Y}_4$($M$=Hg, Cd; Y=S, Se), as well as for metallic local moment systems such as the rare earth metals Gd, Tb, and Dy.[6] The model Hamiltonian consists of three characteristic partial operators,

$$H = H_s + H_f + H_{sf}, \tag{1}$$

concerning the mutual influences of the two well-defined electronic subsystems. H_s stands for itinerant conduction electrons, which are treated as s electrons without explicit Coulomb interaction. At each lattice site $\mathbf{R}$ a permanent magnetic moment is localized represented by a spin operator $\mathbf{S}$. The moment results from an only partially filled electron shell being strictly concentrated to the neighborhood of the respective nucleus ($4f^7$ in Gd, Eu^{2+}). These moments (or spins) exhibit a spontaneous magnetic order below a critical temperature due to a certain (direct or indirect) exchange interaction. That is described by H_f. Many characteristic features of the above mentioned materials may be traced back to an intimate correlation between the two electronic subsystems which is incorporated in the s-f model as an intra-atomic exchange interaction (H_{sf}) between the conduction electron spin σ and the localized f spin $\mathbf{S}$.

Although the s-f model was originally thought to describe the magnetism and the magneto-optic properties of local moment metals and insulators, it also proved to be applicable to a lot of other phenomena in condensed matter physics. It has been used for heavy fermion and mixed valence systems,[7] because of its close relationship to the periodic Anderson model.[8] It will also have a certain relevance to the high T_c problem,[9,10] not only because of its reference to the Anderson model. There is an obvious analogy to the Fröhlich Hamiltonian if one relates the s-f exchange H_{sf} to the electron-phonon interaction and the collective spin excitations (magnons; H_f) to the phonons. Another present day application of the s-f Hamiltonian are the magnetic multilayers, which have been the subject of many recent experimental[11,12] and theoretical[13,14] investigations.

The model Hamiltonian (1) creates a rather sophisticated many body problem that cannot be solved exactly for the general case. We propose in this paper a theory for the special situation of a single electron in an otherwise empty conduction band that interacts via s-f exchange with the ferromagnetically or antiferromagnetically ordered localized spin system.

The study aims at prototypical magnetic semiconductors like the ferromagnet EuO and the antiferromagnet EuTe. Already some 30 years ago it has experimentally been detected that the empty conduction band of EuO exhibits a remarkable temperature dependence. A striking manifestation is the well-known redshift of the optical absorption edge,[4] observed in the meantime for all ferromagnetic semiconductors. A large number of research projects have been focused in the past on this special effect, which can easily be understood for weak exchange couplings within a mean-field approximation. However, the same effect needs a rather different explanation for intermediate or stronger interaction, as will be shown in this paper.

Substantial progress in the understanding of the s-f model has been brought about by the exact solution[15–17] of the special case of a single conduction electron in contact with a ferromagnetically saturated spin system ($T=0$ K). A detailed evaluation[17] reveals rather sophisticated correlation ef-

fects in the energy spectrum. The wave-vector and energy dependent down-spin spectral density consists for not too weak couplings of a sharp quasiparticle peak and a rather broad scattering spectrum. The quasiparticle structure (magnetic polaron) corresponds to a repeated emission and reabsorption of a magnon by the conduction electron resulting in an effective electron-magnon attraction. Under certain conditions, this can even result in a bound state, i.e., a quasiparticle with infinite lifetime. The scattering part is caused by magnon emission of the excited $\downarrow$ electron. Altogether one has to conclude that such features require a careful and unconventional interpretation of respective photoemission experiments. It is the aim of this paper to extend the $T=0$ special case to finite temperatures and different magnetic spin structures. The results are represented in terms of spectral densities, quasiparticle densities of states, and time-dependent quasiparticle propagators. They yield a conclusive impression of the striking consequences of the s-f exchange interaction, the source of many current physical properties of condensed matter.

The paper is organized as follows. In the next section we formulate the many-body problem posed by the s-f Hamiltonian (1). Section III deals with a self-energy approach as the main part of our theory. The special aspects of antiferromagnetic structures are worked out in Sec. IV. The results are presented and discussed in Sec. V. The paper ends with some conclusions and with an outlook concerning applications on real substances.

II. THE s-f PROBLEM

Since we intend to study simultaneously the influence of several magnetic spin structures on the electronic energy spectrum of a magnetic semiconductor, we presume a solid being built up by m penetrating sublattices α ($\alpha=1,2\ldots.m$). The local moments on each of the chemically eqivalent sublattices order ferromagnetically, but possibly with different orientations of the spontaneous magnetization for different α. We refer to the total lattice as a magnetic Bravais lattice ($\mathbf{R}_i$) with an m-atom basis ($\mathbf{r}_\alpha$),

$$\mathbf{R}_{i\alpha}=\mathbf{R}_i+\mathbf{r}_\alpha . \tag{2}$$

i numbers the N sites of the Bravais lattice only. The simplest case is that of a ferromagnet, for which m is equal to 1, so that the sublattice index α becomes meaningless ($\mathbf{r}_\alpha\equiv 0$). In general, translational symmetry can be assumed within a sublattice; i.e., the thermodynamic average of any site-dependent operator $O_{i\alpha}$ is certainly $\mathbf{R}_i$ independent,

$$\langle O_{i\alpha}\rangle=\langle O_\alpha\rangle . \tag{3}$$

There may remain, however, a sublattice dependence. That is why we restrict Fourier transformations to the magnetic lattice and the magnetic Brillouin zone, respectively:

$$O_{i\alpha}=\frac{1}{\sqrt{N}}\sum_{\mathbf{k}} e^{i\mathbf{k}\cdot\mathbf{R}_i}O_{\mathbf{k}\alpha} . \tag{4}$$

Taking into account the sublattice structure, the partial operators of the s-f Hamiltonian (1) read as follows: H_s refers to the conduction electrons being treated as s electrons without Coulomb interaction,

$$H_s=\sum_{ij\sigma,\alpha\beta} T_{ij}^{\alpha\beta}c_{i\alpha\sigma}^\dagger c_{j\beta\sigma}=\sum_{\mathbf{k}\sigma,\alpha\beta}\epsilon_{\alpha\beta}(\mathbf{k})c_{\mathbf{k}\alpha\sigma}^\dagger c_{\mathbf{k}\beta\sigma} . \tag{5}$$

$c_{i\alpha\sigma}^\dagger$ and $c_{i\alpha\sigma}$ are, respectively, the creation and the annihilation operator of an electron with spin σ ($\sigma=\uparrow,\downarrow$) at site $\mathbf{R}_{i\alpha}$. $T_{ij}^{\alpha\beta}$ is the hopping integral and $\epsilon_{\alpha\beta}(\mathbf{k})$ the corresponding Bloch energy,

$$T_{ij}^{\alpha\beta}=\frac{1}{N}\sum_{\mathbf{k}}\epsilon_{\alpha\beta}(\mathbf{k})e^{i\mathbf{k}\cdot(\mathbf{R}_i-\mathbf{R}_j)}. \tag{6}$$

At each lattice site $\mathbf{R}_{i\alpha}$ a permanent magnetic moment is localized, represented by a spin operator $\mathbf{S}_{i\alpha}$. The spin system is described by the Heisenberg model,

$$H_f=-\sum_{ij,\alpha\beta} J_{ij}^{\alpha\beta}\mathbf{S}_{i\alpha}\cdot\mathbf{S}_{j\beta} . \tag{7}$$

$J_{ij}^{\alpha\beta}$ are exchange integrals which are responsible for the magnetic structure. Itinerant electrons and localized spins interact via an intra-atomic exchange H_{sf}:

$$\begin{aligned} H_{sf}&=-J\sum_{j\alpha}\boldsymbol{\sigma}_{j\alpha}\cdot\mathbf{S}_{j\alpha}\\ &=-\frac{1}{2}J\sum_{j\alpha\sigma}(z_\sigma S_{j\alpha}^z n_{j\alpha\sigma}+S_{j\alpha}^\sigma c_{j\alpha-\sigma}^\dagger c_{j\alpha\sigma}). \end{aligned} \tag{8}$$

$\sigma_{j\alpha}$ is the electron spin operator, $n_{j\alpha\sigma}=c_{j\alpha\sigma}^\dagger c_{j\alpha\sigma}$ the occupation number operator, and J the s-f coupling constant. Furthermore, we have introduced for abbreviation

$$S_{j\alpha}^\sigma=S_{j\alpha}^x+iz_\sigma S_{j\alpha}^y ; \quad z_\uparrow=+1,\ z_\downarrow=-1. \tag{9}$$

We investigate in this paper the electronic quasiparticle spectrum of a single electron in an otherwise empty conduction band which interacts with a magnetically ordered localized-spin system. The neglect of any Coulomb interaction in (5) is then trivially justified. Since we are not interested in the purely magnetic properties of the local moment system, we disregard the direct spin-spin interaction H_f [$J_{ij}^{\alpha\beta}\equiv 0$ in (7)]. However, implicitly a spontaneous magnetic order is assumed as will be explained later. For the materials that we are interested in, the s-f exchange coupling J is ferromagnetic ($J>0$). In the case of $J<0$, the model-Hamiltonian (1) is that of the so-called ''Kondo lattice.''[18,19]

All of the information that we want to get can be read off from the retarded single-electron Green function,

$$\begin{aligned} G_{ij\sigma}^{\alpha\beta}(E)&=\langle\langle c_{i\alpha\sigma};c_{j\beta\sigma}^\dagger\rangle\rangle_E\\ &=-i\int_0^\infty dt\,\exp\left(-\frac{i}{\hbar}Et\right)\langle[c_{i\alpha\sigma}(t),c_{j\beta\sigma}^\dagger(0)]_+\rangle . \end{aligned} \tag{10}$$

Here and in the following $[\ldots,\ldots]_+$ ($[\ldots,\ldots]_-$) means the anticommutator (commutator). The equation of motion of the Green function reads

$$\sum_{r\gamma}(E\delta_{ir}\delta_{\alpha\gamma}-T_{ir}^{\alpha\gamma})G_{rj\sigma}^{\gamma\beta}(E) = \hbar\delta_{ij}\delta_{\alpha\beta}+\langle\langle[c_{i\alpha\sigma},H_{sf}]_-;c_{j\beta\sigma}^{\dagger}\rangle\rangle_E. \quad (11)$$

The introduction of the self-energy matrix $M_{ij\sigma}^{\alpha\beta}(E)$,

$$\langle\langle[c_{i\alpha\sigma},H_{sf}]_-;c_{j\beta\sigma}^{\dagger}\rangle\rangle_E \doteq \sum_{r\gamma} M_{ir\sigma}^{\alpha\gamma}(E)G_{rj\sigma}^{\gamma\beta}(E), \quad (12)$$

formally solves the problem. After Fourier transformation according to (4), it remains that

$$\sum_{\gamma}[E\delta_{\alpha\gamma}-\epsilon_{\alpha\gamma}(\mathbf{k})-M_{\mathbf{k}\sigma}^{\alpha\gamma}(E)]G_{\mathbf{k}\sigma}^{\gamma\beta}(E)=\hbar\delta_{\alpha\beta}. \quad (13)$$

The self-energy $M_{\mathbf{k}\sigma}^{\alpha\beta}(E)$ gathers all influences of the s-f exchange interaction being therefore the central quantity of our study.

A function of exactly the same usefulness as the Green function $G_{\mathbf{k}\sigma}^{\alpha\beta}(E)$ is the single-electron spectral density being directly related, except for a respective dipole-transition matrix element, to an angle- and spin-resolved (inverse) photoemission experiment,

$$S_{\mathbf{k}\sigma}^{\alpha\beta}(E)=-\frac{1}{\pi}\mathrm{Im}\,G_{\mathbf{k}\sigma}^{\alpha\beta}(E+i0^+). \quad (14)$$

An additional wave-vector summation yields the (sublattice) quasiparticle density of states, in terms of which we shall partly discuss our results,

$$\rho_{\alpha\sigma}(E)=\frac{1}{N\hbar}\sum_{\mathbf{k}} S_{\mathbf{k}\sigma}^{\alpha\alpha}(E). \quad (15)$$

In the next section, we evaluate the electron self-energy first for a ferromagnetic semiconductor.

III. SELF-ENERGY APPROACH (FERROMAGNETS)

In the case of a ferromagnetic semiconductor the total system possesses translational symmetry. In the formalism of Sec. II that means $m=1$, $\mathbf{r}_\alpha=0$. The sublattice indices α, β become meaningless and are suppressed in the following.

The starting point is the equation of motion of the single-electron Green function (11). Evaluating explicitly the commutator $[c_{i\alpha\sigma},H_{sf}]_-$ leads to

$$\sum_r(E\delta_{ir}-T_{ir})G_{rj\sigma}(E) = \hbar\delta_{ij}-\frac{1}{2}J[z_\sigma\Gamma_{ii,j\sigma}(E)+F_{ii,j\sigma}(E)]. \quad (16)$$

Two higher Green functions appear on the right hand side, which we call the spin-flip function,

$$F_{ip,j\sigma}(E)=\langle\langle S_i^{-\sigma}c_{p-\sigma};c_{j\sigma}^{\dagger}\rangle\rangle_E, \quad (17)$$

and the ''Ising function,'' respectively:

$$\Gamma_{ip,j\sigma}(E)=\langle\langle S_i^z c_{p\sigma};c_{j\sigma}^{\dagger}\rangle\rangle_E. \quad (18)$$

These functions prevent a direct solution of the equation of motion (16). To proceed, we construct in the next step the equation of motion of the higher functions (17) and (18):

$$\sum_r(E\delta_{pr}-T_{pr})F_{ir,j\sigma}(E)=\langle\langle S_i^{-\sigma}[c_{p-\sigma},H_{sf}]_-;c_{j\sigma}^{\dagger}\rangle\rangle_E, \quad (19)$$

$$\sum_r(E\delta_{pr}-T_{pr})\Gamma_{ir,j\sigma}(E) = \hbar\langle S^z\rangle\delta_{pj}+\langle\langle S_i^z[c_{p\sigma},H_{sf}]_-;c_{j\sigma}^{\dagger}\rangle\rangle_E. \quad (20)$$

Because of the empty energy band,

$$\langle n_{i\sigma}\rangle=\langle n_\sigma\rangle=0, \quad (21)$$

the Green functions

$$\langle\langle[S_i^{-\sigma},H_{sf}]_-c_{p-\sigma};c_{j\sigma}^{\dagger}\rangle\rangle,$$

$$\langle\langle[S_i^z,H_{sf}]_-c_{p\sigma};c_{j\sigma}^{\dagger}\rangle\rangle,$$

which, in principle, appear in (19) and (20), respectively, are identical to zero. The treatment of the two other new functions in (19) and (20) consists of two steps, since strong local correlations require a special treatment when spin and electron operators act at the same site ($i=p$). We first discuss, however, the nondiagonal terms ($i\neq p$).

A. $i\neq p$

The starting point is to define Eq. (12) for the electronic self-energy, which formally corresponds to the replacement

$$[c_{i\sigma},H_{sf}]_-\Rightarrow\sum_r M_{ir\sigma}(E)c_{r\sigma} \quad (22)$$

within the brackets of the Green function. The inspection of the spectral representations[20] of the two functions in (12), $\langle\langle[c_{i\sigma},H_{sf}]_-;c_{j\sigma}^{\dagger}\rangle\rangle_E$ and $\langle\langle c_{i\sigma};c_{j\sigma}^{\dagger}\rangle\rangle$, reveals that both must have the same pole structure and can differ only by the spectral weights of the poles. The equality of both sides in (12) is installed by the self-energy components $M_{ir\sigma}(E)$. If we now inspect, under the same aspect, the spectral decomposition of the following two functions,

$$\langle\langle S_i^z[c_{p\sigma},H_{sf}]_-;c_{j\sigma}^{\dagger}\rangle\rangle_E;\quad \langle\langle S_i^z c_{r\sigma};c_{j\sigma}^{\dagger}\rangle\rangle,$$

then we come again to the conclusion that they can differ only by their spectral weights, but must have the same pole structure. In analogy to (12) we, therefore, propose to use (22) in these functions, too:

$$\langle\langle S_i^z[c_{p\sigma},H_{sf}]_-;c_{j\sigma}^{\dagger}\rangle\rangle_E \approx \sum_r M_{pr\sigma}(E)\langle\langle S_i^z c_{r\sigma};c_{j\sigma}^{\dagger}\rangle\rangle_E \quad (i\neq p). \quad (23)$$

The same justification can be used for

$$\langle\langle S_i^{-\sigma}[c_{p-\sigma},H_{sf}]_-;c_{j\sigma}^{\dagger}\rangle\rangle_E \approx \sum_r M_{pr-\sigma}(E)\langle\langle S_i^{-\sigma}c_{r-\sigma};c_{j\sigma}^{\dagger}\rangle\rangle_E \quad (i\neq p). \tag{24}$$

For $i\neq p$ the equations (16)–(20), (23), and (24) build a closed system. For $i=p$ we have to use another procedure which takes stronger into account the local correlations.

B. $i=p$

We start with an explicit evaluation of the commutator in the higher Green functions on the right hand sides of (19) and (20). The higher spin-flip function in (19) yields for $i=p$,

$$\langle\langle S_i^{-\sigma}[c_{i-\sigma},H_{sf}]_-;c_{j\sigma}^{\dagger}\rangle\rangle = \tfrac{1}{2}J[z_\sigma F_{ii,j\sigma}^{(1)}(E)-F_{ii,j\sigma}^{(2)}(E)]. \tag{25}$$

Here we have abbreviated

$$F_{ii,j\sigma}^{(1)}(E)=\langle\langle S_i^{-\sigma}S_i^z c_{i-\sigma};c_{j\sigma}^{\dagger}\rangle\rangle_E, \tag{26}$$

$$F_{ii,j\sigma}^{(2)}(E)=\langle\langle S_i^{-\sigma}S_i^{\sigma} c_{i\sigma};c_{j\sigma}^{\dagger}\rangle\rangle_E. \tag{27}$$

The analogous evaluation of the higher Ising function in (20) for $i=p$ does not require the introduction of further Green functions, because it can exactly be expressed by already defined terms:

$$\langle\langle S_i^z[c_{i\sigma},H_{sf}]_-;c_{j\sigma}^{\dagger}\rangle\rangle + z_\sigma\langle\langle S_i^{-\sigma}[c_{i-\sigma},H_{sf}]_-;c_{j\sigma}^{\dagger}\rangle\rangle = \tfrac{1}{2}J[\Gamma_{ii,j\sigma}(E)+z_\sigma F_{ii,j\sigma}(E)]-\tfrac{1}{2}Jz_\sigma S(S+1)G_{ij\sigma}(E), \tag{28}$$

(25) and (28) are still exact. To get a closed system of equations for $i=p$, too, we are left with the determination of the functions $F_{ii,j\sigma}^{(1,2)}(E)$. Both fulfill some important exact relations. For $S=1/2$ it holds for all temperatures:

$$F_{ii,j\sigma}^{(1)}(E)=\tfrac{1}{2}z_\sigma F_{ii,j\sigma}(E), \tag{29}$$

$$F_{ii,j\sigma}^{(2)}(E)=\tfrac{1}{2}G_{ij\sigma}(E)-z_\sigma\Gamma_{ii,j\sigma}(E). \tag{30}$$

The same two functions for arbitrary spin S, but in the ferromagnetic saturation ($\langle S^z\rangle=S$) are given by

$$F_{ii,j\sigma}^{(1)}(E)\rightarrow[(S-\tfrac{1}{2})+\tfrac{1}{2}z_\sigma]F_{ii,j\sigma}(E), \tag{31}$$

$$F_{ii,j\sigma}^{(2)}(E)\rightarrow SG_{ij\sigma}(E)-z_\sigma\Gamma_{ii,j\sigma}(E). \tag{32}$$

These exact relationships suggest the following general structures:

$$F_{ii,j\sigma}^{(1)}(E)=\alpha_{1\sigma}G_{ij\sigma}(E)+\beta_{1\sigma}F_{ii,j\sigma}(E), \tag{33}$$

$$F_{ii,j\sigma}^{(2)}(E)=\alpha_{2\sigma}G_{ij\sigma}(E)+\beta_{2\sigma}\Gamma_{ii,j\sigma}(E). \tag{34}$$

The five Green functions in (33) and (34) are of the same type $\langle\langle A;B\rangle\rangle_E$. For each of them we can calculate exactly the first two spectral moments according to the relation

$$M_{AB}^{(n)}=\left\langle\left(i\hbar\frac{\partial}{\partial t}\right)^n[A(t),B(0)]_+\right\rangle_{t=0}, \quad n=0,1,2\ldots. \tag{35}$$

Because of the equivalent relation

$$M_{AB}^{(n)}=-\frac{1}{\pi\hbar}\int_{-\infty}^{\infty}dE\ E^n\,\mathrm{Im}\langle\langle A,B\rangle\rangle_E, \tag{36}$$

the moments can be used to fix the coefficients $\alpha_{m\sigma}$, $\beta_{m\sigma}$ in (33) and (34). After tedious but straightforward manipulations, we get

$$\alpha_{1\sigma}=0; \quad \beta_{1\sigma}=\frac{\langle S^{-\sigma}S^{\sigma}S^z\rangle+z_\sigma\langle S^{-\sigma}S^{\sigma}\rangle}{\langle S^{-\sigma}S^{\sigma}\rangle}, \tag{37}$$

$$\alpha_{2\sigma}=\langle S^{-\sigma}S^{\sigma}\rangle-\beta_{2\sigma}\langle S^z\rangle, \tag{38}$$

$$\beta_{2\sigma}=\frac{\langle S^{-\sigma}S^{\sigma}S^z\rangle-\langle S^z\rangle\langle S^{-\sigma}S^{\sigma}\rangle}{\langle(S^z)^2\rangle-\langle S^z\rangle^2}. \tag{39}$$

The coefficients are determined by f-spin correlation functions, the determination of which has to be considered at a later stage of our procedure.

The equations (16), (19), (20), (23)–(25), (33), (34), and (37)–(39) build a closed system, which can be solved self-consistently for the single-electron Green function:

$$G_{\mathbf{q}\sigma}(E)=\hbar[E-\epsilon(\mathbf{q})-M_{\mathbf{q}\sigma}(E)]^{-1}. \tag{40}$$

The solution becomes possible by Fourier transformation,

$$G_{\mathbf{q}\sigma}(E)=\frac{1}{N}\sum_{i,j}G_{ij\sigma}(E)e^{-i\mathbf{q}\cdot(\mathbf{R}_i-\mathbf{R}_j)}, \tag{41}$$

$$A_{\mathbf{kp},\mathbf{q}\sigma}(E)=\frac{1}{N^2}\sum_{ijm}A_{im,j\sigma}(E)e^{-i(\mathbf{k}\cdot\mathbf{R}_i+\mathbf{p}\cdot\mathbf{R}_m-\mathbf{q}\cdot\mathbf{R}_j)} \quad (A=F,\Gamma). \tag{42}$$

In addition, we can exploit translational symmetry

$$A_{\mathbf{kp},\mathbf{q}\sigma}(E)=\delta_{\mathbf{k}+\mathbf{p},\mathbf{q}}A_{\mathbf{q}-\mathbf{p}\ \mathbf{p},\mathbf{q}\sigma}(E). \tag{43}$$

The evaluation yields a wave-vector independent electronic self-energy,

$$M_{\mathbf{q}\sigma}(E)\equiv M_\sigma(E)=-\frac{1}{2}Jm_\sigma(E). \tag{44}$$

The reason of the **q** independence can be traced back to the neglect of magnon energies. Spin flips of the conduction electrons may be accompanied by magnon emission or absorption. Since we agreed upon setting $H_f=0$, the wave vector and energy dependence of the magnon energies $\hbar\omega(\mathbf{q})$ do not enter our results. Since magnon energies are smaller by two or three orders of magnitude than typical electronic energies, as, for instance, the coupling constant J and the bandwidth W, such a neglect appears to be allowed. For the self-energy we eventually get the following implicit equation:

$$m_\sigma(E)=\frac{Q_\sigma(E)}{N_\sigma(E)}, \tag{45}$$

$$\begin{aligned}Q_\sigma(E)=&z_\sigma\langle S^z\rangle+\tfrac{1}{2}J\{[\alpha_{2\sigma}-S(S+1)]G_{0\sigma}(E)-[\alpha_{2\sigma}\\&+\langle S^z\rangle(\beta_{1\sigma}+\beta_{2\sigma})-z_\sigma\langle S^z\rangle m_{-\sigma}(E)]G_{0-\sigma}(E)\}\\&+\tfrac{1}{4}J^2\{z_\sigma S(S+1)(\beta_{1\sigma}+\beta_{2\sigma})-\alpha_{2\sigma}m_\sigma(E)\\&+[\alpha_{2\sigma}-S(S+1)]m_{-\sigma}(E)\}G_{0\sigma}(E)G_{0-\sigma}(E),\end{aligned} \tag{46}$$

$$\begin{aligned}N_\sigma(E)=&1+\tfrac{1}{2}J\{[m_\sigma(E)-1-z_\sigma\beta_{2\sigma}]G_{0\sigma}(E)+[m_{-\sigma}(E)\\&-z_\sigma\beta_{1\sigma}]G_{0-\sigma}(E)\}+\tfrac{1}{4}J^2\{[m_\sigma(E)-1-z_\sigma\beta_{2\sigma}]\\&\times[m_{-\sigma}(E)-z_\sigma\beta_{1\sigma}]+\beta_{2\sigma}(\beta_{1\sigma}-z_\sigma)\}\\&\times G_{0\sigma}(E)G_{0-\sigma}(E).\end{aligned} \tag{47}$$

One recognizes immediately that the first-order expression coincides with the well-known mean-field result, valid for very weak s-f exchange couplings:

$$M_\sigma^{(1)}(E)=-\tfrac{1}{2}Jz_\sigma\langle S^z\rangle. \tag{48}$$

In (46) and (47) appears the propagator:

$$G_{0\sigma}(E)=\frac{1}{N}\sum_{\mathbf{q}}G_{\mathbf{q}\sigma}(E)=\int_{-\infty}^{\infty}dx\,\frac{\rho_0(x)}{E-x-M_\sigma(E)}. \tag{49}$$

$\rho_0(x)$ is the Bloch density of states of the ''free'' conduction electron system, which of course depends on the lattice structure. We have evaluated our theory for a simple cubic structure. Electron hopping is taken into account for the nearest (T_1) and next nearest (T_2) neighbor hopping:

$$\epsilon(\mathbf{k})=T_0+T_1f_1(\mathbf{k})+T_2f_2(\mathbf{k}), \tag{50}$$

$$f_1(\mathbf{k})=2[\cos(k_xa)+\cos(k_ya)+\cos(k_za)], \tag{51}$$

$$\begin{aligned}f_2(\mathbf{k})=&2\{\cos[(k_x+k_y)a]+\cos[(k_x+k_z)a]\\&+\cos[(k_y+k_z)a]+\cos[(k_x-k_y)a]\\&+\cos[(k_x-k_z)a]+\cos[(k_y-k_z)a]\}.\end{aligned} \tag{52}$$

The Bloch energies $\epsilon(\mathbf{k})$ are plotted in Fig. 1 for certain symmetry directions as well as the Bloch density of states $\rho_0(E)$.

For the concrete evaluation we have chosen

$$T_0=0;\quad T_1=-0.05;\quad T_2=T_1/\sqrt{2}. \tag{53}$$

The self-energy (45)–(47) is strongly influenced by the coefficients $\alpha_{2\sigma}$, $\beta_{1\sigma}$, $\beta_{2\sigma}$, where these quantities are pure f-spin correlation functions according to (37)–(39). We did not explicitly take into account the direct interaction between the localized f spins. We agreed to consider the spontaneous magnetization $\langle S^z\rangle$ as a given temperature-dependent parameter. The f-spin correlations in (37)–(39) can be determined by the pure Heisenberg model, since the assumed empty conduction band has no influence on the magnetic properties of the spin system. It can be shown[21] that the magnetization $\langle S^z\rangle$ obeys the following formula:[22]

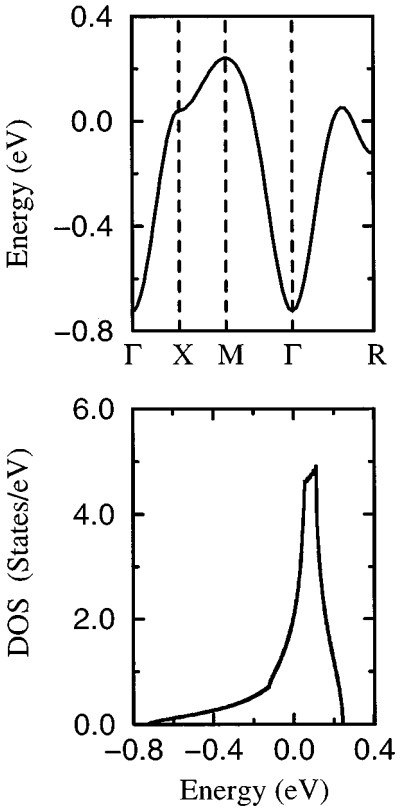

FIG. 1. Bloch band structure and density of states for a simple cubic lattice in a tight-binding approximation with nearest and next nearest neighbor hopping [parameters in (53)].

$$\langle S^z\rangle=\hbar\frac{(1+S+\varphi)\varphi^{2S+1}+(S-\varphi)(1+\varphi)^{2S+1}}{(1+\varphi)^{2S+1}-\varphi^{2S+1}}, \tag{54}$$

provided the single-magnon Green function is a one-pole function at the real magnon energy $E(\mathbf{q})$:

$$\varphi=\varphi(S)=\frac{1}{N}\sum_{\mathbf{q}}(e^{\beta E(\mathbf{q})}-1)^{-1}. \tag{55}$$

Equation (54) holds for arbitrary spin values. Furthermore one finds the very useful relations[21]

$$\langle S^-S^+\rangle=2\hbar\langle S^z\rangle\varphi(S), \tag{56}$$

$$\langle(S^z)^2\rangle=\hbar^2S(S+1)-\hbar\langle S^z\rangle[1+2\varphi(S)], \tag{57}$$

$$\begin{aligned}\langle(S^z)^3\rangle=&\hbar^3S(S+1)\varphi(S)+\hbar^2\langle S^z\rangle[S(S+1)+\varphi(S)]\\&-\hbar\langle(S^z)^2\rangle[1+3\varphi(S)],\end{aligned} \tag{58}$$

so that lastly the coefficients in (37)–(39) are expressed in terms of φ. Our procedure is as follows. We consider $\langle S^z\rangle$ as a given parameter to which we ascribe by use of (54) a certain $\varphi(S)$. That $\varphi(S)$ helps to derive the other spin correlation functions. Figure 2 shows some examples.

The self-energy (44) turns out to be, in general, a complex quantity

$$M_\sigma(E)=R_\sigma(E)+iI_\sigma(E). \tag{59}$$

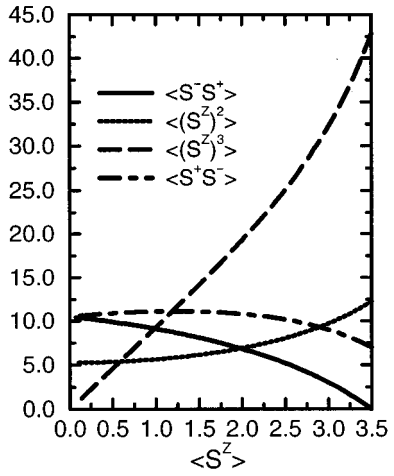

FIG. 2. Correlation functions of the localized-spin system as a function of the magnetization $\langle S^z\rangle$ ($S=7/2$).

According to (14) and (40) the spectral density of the ferromagnet is then given by

$$S_{\mathbf{k}\sigma}(E)=-\frac{1}{\pi}\mathrm{Im}\,G_{\mathbf{k}\sigma}(E)$$

$$=-\frac{\hbar}{\pi}\frac{I_\sigma(E)}{[E-\epsilon(\mathbf{k})-R_\sigma(E)]^2+I_\sigma^2(E)}. \tag{60}$$

An additional wave-vector summation yields the quasiparticle density of states (QDOS),

$$\rho_\sigma(E)=\frac{1}{N\hbar}\sum_{\mathbf{k}} S_{\mathbf{k}\sigma}(E). \tag{61}$$

IV. SELF-ENERGY APPROACH (ANTIFERROMAGNETS)

We now assume a two sublattice structure (α, β:A, B), where each sublattice orders ferromagnetically but with different directions of the spontaneous magnetization. The starting point is again equation (13) which reads in a matrix representation

$$\hat{G}_{\mathbf{k}\sigma}(E)=\hbar[E-\hat{\epsilon}(\mathbf{k})-\hat{M}_{\mathbf{k}\sigma}(E)]^{-1}. \tag{62}$$

Because of chemically totally equivalent sublattices it holds for the elements of the Bloch matrix $\hat{\epsilon}(\mathbf{k})$,

$$\epsilon_{AA}(\mathbf{k})=\epsilon_{BB}(\mathbf{k})\equiv\epsilon(\mathbf{k}), \tag{63}$$

$$\epsilon_{AB}(\mathbf{k})=\epsilon^*_{BA}(\mathbf{k})\equiv t(\mathbf{k}). \tag{64}$$

That means

$$\hat{\epsilon}(\mathbf{k})=\begin{pmatrix}\epsilon(\mathbf{k}) & t(\mathbf{k})\\ t^*(\mathbf{k}) & \epsilon(\mathbf{k})\end{pmatrix}. \tag{65}$$

Similar symmetry relations are valid for the self-energy matrix:

$$M^{AA}_{\mathbf{k}\sigma}(E)=M^{BB}_{\mathbf{k}-\sigma}\equiv M_{\mathbf{k}\sigma}(E), \tag{66}$$

$$M^{AB}_{\mathbf{k}\sigma}(E)=M^{BA*}_{\mathbf{k}\sigma}\equiv T_{\mathbf{k}}(E). \tag{67}$$

That means

$$\hat{M}_{\mathbf{k}\sigma}(E)=\begin{pmatrix}M_{\mathbf{k}\sigma}(E) & T_{\mathbf{k}}(E)\\ T^*_{\mathbf{k}}(E) & M_{\mathbf{k}-\sigma}(E)\end{pmatrix}. \tag{68}$$

Matrix inversion in (62) yields

$$\hat{G}_{\mathbf{k}\sigma}(E)$$

$$=\frac{\hbar}{\Delta_{\mathbf{k}}(E)}\begin{pmatrix}E-\epsilon(\mathbf{k})-M_{\mathbf{k}-\sigma}(E) & t(\mathbf{k})+T_{\mathbf{k}}(E)\\ t^*(\mathbf{k})+T^*_{\mathbf{k}}(E) & E-\epsilon(\mathbf{k})-M_{\mathbf{k}\sigma}(E)\end{pmatrix}, \tag{69}$$

$$\Delta_{\mathbf{k}}(E)=[E-\epsilon(\mathbf{k})-M_{\mathbf{k}\sigma}(E)][E-\epsilon(\mathbf{k})-M_{\mathbf{k}-\sigma}(E)]$$

$$-|t(\mathbf{k})+T_{\mathbf{k}}(E)|^2. \tag{70}$$

The sublattice spectral density of the antiferromagnet is then given by

$$S^{AA}_{\mathbf{k}\sigma}(E)=-\frac{1}{\pi}\mathrm{Im}\frac{E-\epsilon(\mathbf{k})-M_{\mathbf{k}-\sigma}(E)}{\Delta_{\mathbf{k}}(E)}=S^{BB}_{\mathbf{k}-\sigma}(E). \tag{71}$$

We remember that $\mathbf{k}$ is a wave vector from the first Brillouin zone of the magnetic Bravais lattice, i.e., of the (ferromagnetic) sublattice. The angle- and spin-resolved photoemission experiment observes the single-electron spectral density. Strictly speaking, the mentioned (inverse) photoemission experiment refers to the total chemical lattice. If $\mathbf{q}$ is from the first Brillouin zone of the total lattice, then the following simple relation holds:

$$S_{\mathbf{q}}(E)=\frac{1}{2}\sum_{\alpha} S^{\alpha\alpha}_{\mathbf{q}+\mathbf{K}\sigma}(E)+S^{AB}_{\mathbf{q}+\mathbf{K}}(E)\cos[\mathbf{q}\cdot(\mathbf{r}_A-\mathbf{r}_B)]. \tag{72}$$

The observed spectral density of the two-sublattice antiferromagnet is of course spin independent. $\mathbf{K}$ is just the reciprocal lattice vector which transfers $\mathbf{q}$ into the first Brillouin zone of the magnetic Bravais lattice.

A further quantity of importance is the sublattice quasiparticle density of states,

$$\rho_{\alpha\sigma}(E)=\frac{1}{N}\sum_{\mathbf{k}} S^{\alpha\alpha}_{\mathbf{k}\sigma}(E),\quad \alpha=A,B. \tag{73}$$

The nondiagonal element $T_{\mathbf{k}}(E)$ of the self-energy matrix (68) disappears at temperatures above the Néel-temperature T_N. Our approximation consists in the assumption that $T_{\mathbf{k}}(E)$ can be neglected for all temperatures and that the self-energy part $M_{\mathbf{k}\sigma}(E)$ of the respective ferromagnetic sublattice has the same structure (44) as that of a ferromagnetic semiconductor. This assumption is realistic and acceptable and has been justified in Ref. 23 for the Hubbard model.

To allow a direct comparison to the ferromagnetic counterpart (Sec. III), we evaluate our theory again for a simple cubic lattice, which is decomposed into two sublattices in such a way that the nearest neighbors of each atom are from the other sublattice. As in (50), we have taken into consideration the nearest and next nearest hopping. That means

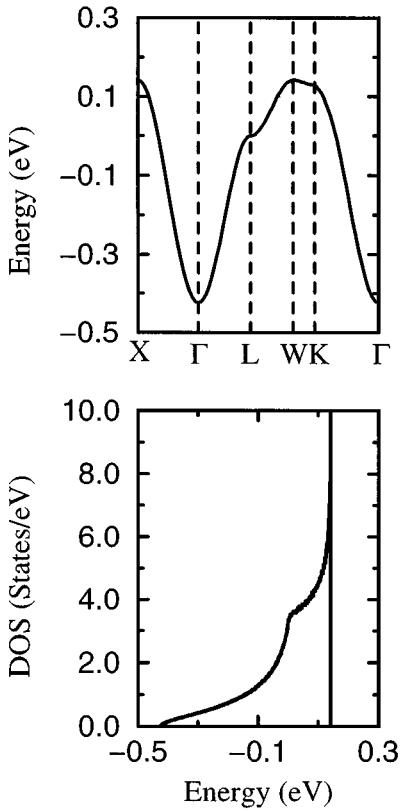

FIG. 3. Bloch-band structure and density of states for the fcc sublattice of an antiferromagnetically ordered sc lattice in a tight-binding approximation with nearest and next nearest neighbor hopping [parameters in (53)].

$$\epsilon(\mathbf{k}) = T_0 + 2T_2\Big[\cos\Big((k_x+k_y)\frac{a}{2}\Big) + \cos\Big((k_x+k_z)\frac{a}{2}\Big) + \cos\Big((k_y+k_z)\frac{a}{2}\Big) + \cos\Big((k_x-k_y)\frac{a}{2}\Big) + \cos\Big((k_x-k_z)\frac{a}{2}\Big) + \cos\Big((k_y-k_z)\frac{a}{2}\Big)\Big] \tag{74}$$

$$t(\mathbf{k}) = 2T_1\Big[\cos\Big(k_x\frac{a}{2}\Big) + \cos\Big(k_y\frac{a}{2}\Big) + \cos\Big(k_z\frac{a}{2}\Big)\Big]. \tag{75}$$

The wave vector $\mathbf{k}=(k_x,\ k_y,\ k_z)$ is now from the first Brillouin zone of the fcc-magnetic Bravais lattice. The hopping constants T_0, T_1, T_2 are same as in (53). The Bloch band structure and the corresponding density of states of the fcc sublattice are shown in Fig. 3. As to the f-spin correlations, we assume the same relation (54), only $\varphi(S)$ has to be reinterpreted and all entities are sublattice entities. Since $\langle S_\alpha^z\rangle$ is our primary parameter, the different meaning of $\varphi(S)$ does not affect our procedure. From a given sublattice magnetization $\langle S_\alpha^z\rangle$, we determine via Eq. (54) the corresponding $\varphi(S)$ and therewith all spin correlations necessary for our theory [(56)–(58)].

V. DISCUSSION OF THE RESULTS

We have evaluated our theory for a simple cubic lattice where the electron hopping is taken into account up to nearest and next nearest neighbors. The corresponding Bloch energies $\epsilon(\mathbf{k})$ are given in (50) for the crystal without and in (73), (74) for the crystal with sublattice decomposition. Our interest is mainly focused on correlation and temperature effects in the energy spectrum of the single conduction electron as a consequence of its exchange coupling to the localized-spin system. The (sublattice) magnetization $\langle S^z\rangle$ ($\langle S_\alpha^z\rangle$) is considered as a given parameter. Temperature comes into play excludingly via $\langle S^z\rangle$ and some other spin correlations (37)–(39), where, however, the latter are expressible by $\langle S^z\rangle$ [see Eqs. (56)–(58)]. The Bloch bandwidth is fixed by the parameter choice (53) and the spin value of the f system is chosen to $S=7/2$.

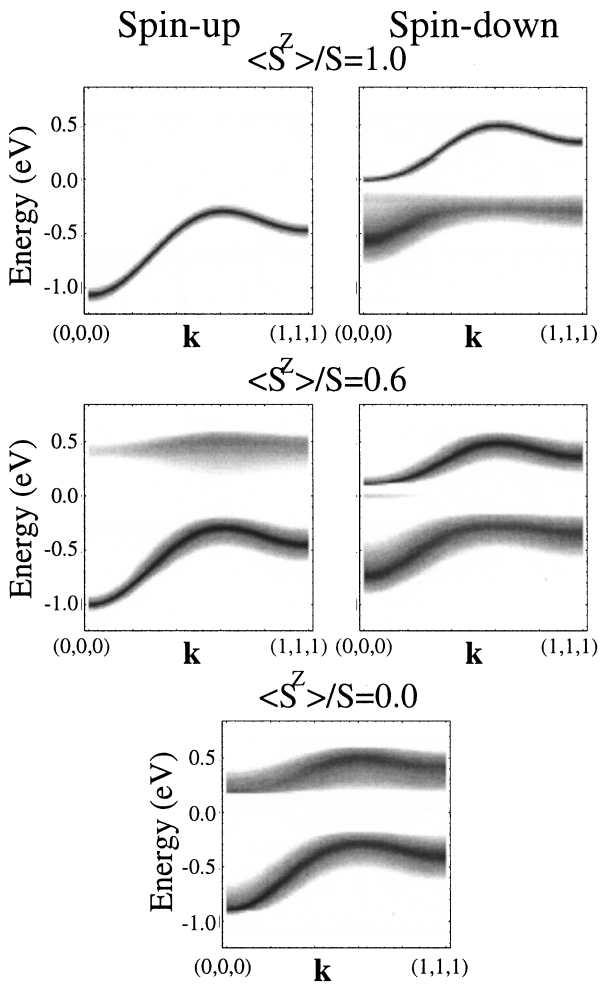

FIG. 4. Density plot of the spectral density of the ferromagnetic semiconductor as function of energy for wave vectors from the (111) direction and for both spin projections. The degree of blackening measures the magnitude of the spectral density. Results are plotted for three different magnetizations of the ferromagnetic f-spin system (parameters: $J=0.2$ eV, $S=7/2$, sc lattice).

A. Ferromagnet

In a ferromagnetically saturated spin system ($T=0$; $\langle S^z\rangle = S$) an $\uparrow$-spin electron cannot exchange its spin. The spin-flip terms of the s-f interaction [second term in (8)] do not work, only the Ising-like term $z_\sigma S_j^z n_{j\sigma}$ takes care for a rigid shift of the quasiparticle energies $E_\uparrow(\mathbf{k})$ compared to the Bloch energies $\epsilon(\mathbf{k})$,

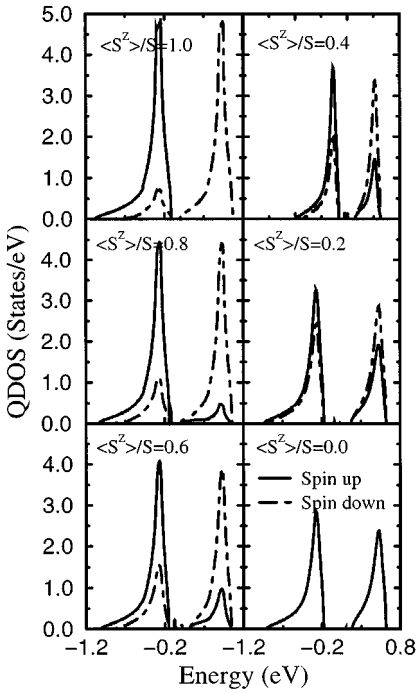

FIG. 5. Quasiparticle density of states $\rho_\sigma(E)$ of the conduction band of the ferromagnetic semiconductor as function of energy for various values of the f-spin magnetization. Full line for $\sigma=\uparrow$ and broken line for $\sigma=\downarrow$. Parameters as in Fig. 4.

$$E_\uparrow(\mathbf{k})=\epsilon(\mathbf{k})-\tfrac{1}{2}JS. \tag{76}$$

The up-spin spectral density (60) is a single δ function corresponding to a quasiparticle with infinite lifetime. This is represented in Fig. 4, where we have plotted the spectral density $S_{\mathbf{k}\sigma}(E)$ for wave vectors from the (111) direction as a function of energy in the form of a density plot. The degree of blackening measures the magnitude of $S_{\mathbf{k}\sigma}(E)$. For plotting convenience, we have added a small imaginary part to the self-energy giving the spectral density a small finite width. Equation (76) is a simple but exact result.[17] This holds also for the down-spin spectral density in the case of ferromagnetic saturation $\langle S^z\rangle=S$. However, the down-spin quasiparticle spectrum is far from being trivial. For the coupling strength $J=0.2$ eV, used in Fig. 4, it consists of two prominent structures which should be observable in a respective inverse photoemission experiment. Both structures may be understood on the basis of a repeated emission and absorption of magnons by the electron. The upper part refers to an effective attraction between magnon and electron resulting in a polaronlike quasiparticle (electron plus magnon cloud). It manifests itself as a pole of the single-electron Green function. We call this quasiparticle excitation the magnetic polaron. At $\langle S^z\rangle=S$ and strong enough J, it is even a bound state coming out as a δ function in the spectral density. For weak J the polaron dispersion dips into the region, where $\uparrow$ states exist $[\rho_\uparrow(E)\neq 0]$. Then the polaron may decay into a $\uparrow$ electron and a magnon, the quasiparticle peak is therewith getting a finite width. A direct emission of a magnon by the excited down-spin electron leads to the second structure in $S_{\mathbf{k}\downarrow}(E)$ (Fig. 4). Magnon emission by the down-spin electron becomes possible always if there are $\uparrow$ states within the

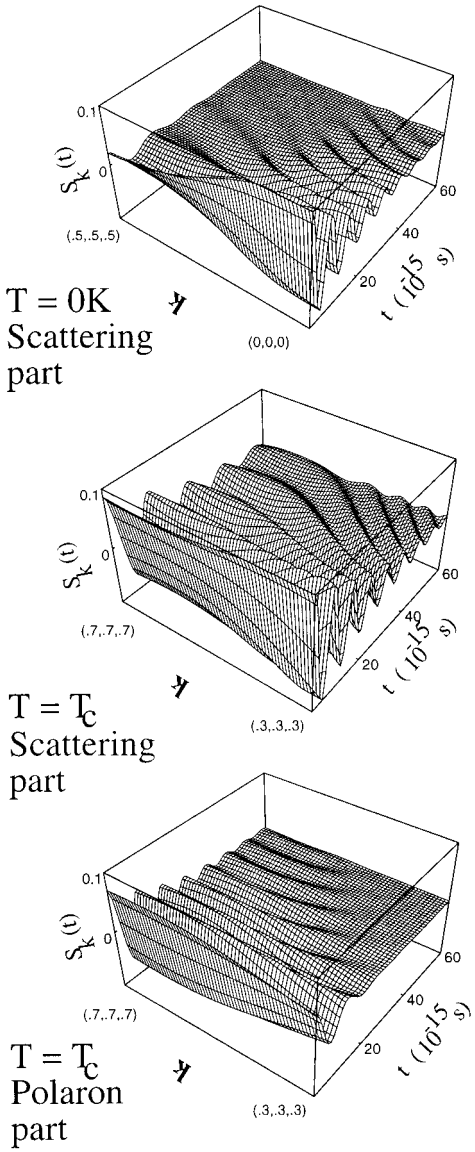

FIG. 6. Time-dependent propagator $S_{\mathbf{k}\sigma}(t)$ [Fourier transform of $S_{\mathbf{k}\sigma}(E)$] as function of time for various wave vectors from the (111) direction. The upper part belongs to the scattering (low energy) peak of the $\downarrow$-spectral density in the ferromagnetic saturation (Fig. 4: $\langle S^z\rangle/S=1$). The middle part is the Fourier transform of the scattering part in the spectral density at $T=T_c$ (Fig. 4: $\langle S^z\rangle/S=0$), while the lower part represents the magnetic polaron at $T=T_c$. Parameters as in Fig. 4.

reach for the electron to land after the spin flip. Since we neglected magnon energies $[\hbar\omega(\mathbf{q})=0]$ from the very beginning, the scattering spectrum of the $\downarrow$-spin electron therefore stretches over the full region of finite up-spin density of states (Fig. 5). However, in most cases the scattering states are bunched together to a pronounced peak. To both peaks can be ascribed a spectral weight that scales with the area under the respective peak. The total weight of the $(\mathbf{k},\sigma)$-dependent spectral density is normalized to one. The relative weight of the polaron peak compared to that of the scattering part appears to be strongly dependent on the position in the Brillouin zone. We stress once more that the $\langle S^z\rangle=S$ results are exact.

Magnon emission by a down-spin electron should be

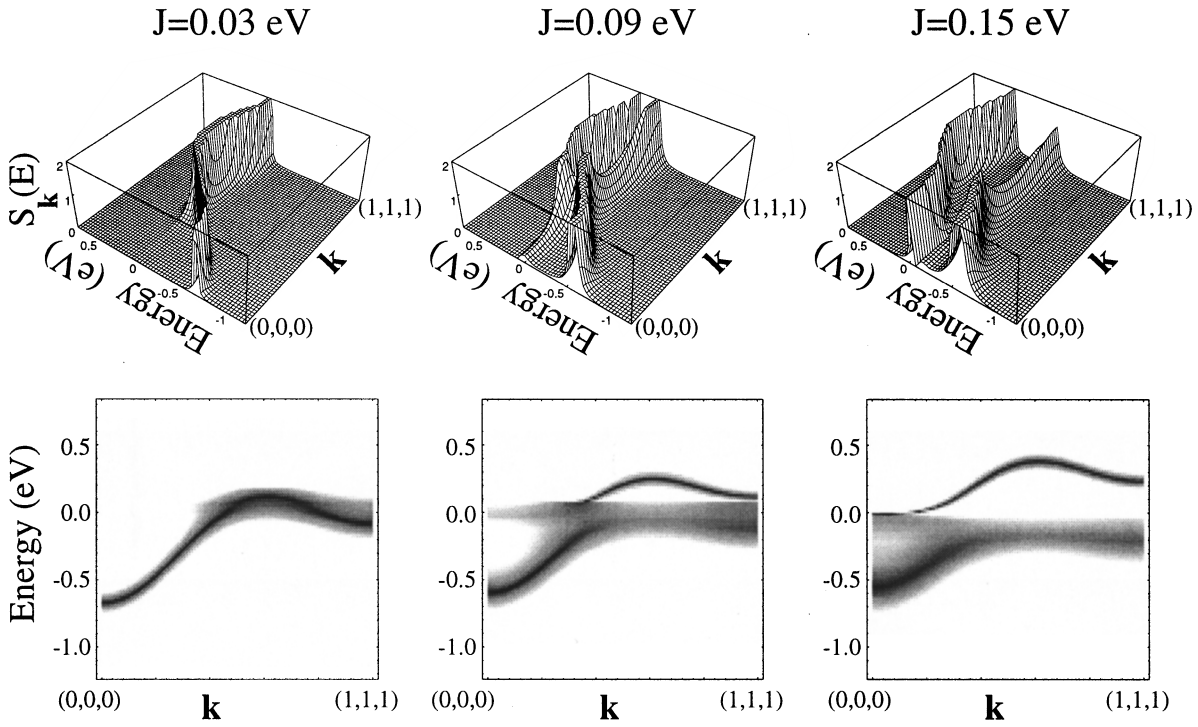

FIG. 7. Down-spin spectral density $S_{\mathbf{k}\downarrow}(E)$ of the ferromagnetic semiconductor at $T=0$ K ($\langle S^z\rangle/S=1$) as function of energy for wave vectors from the (111) direction. Each plot belongs to another s-f exchange coupling (exact results). Other parameters as in Fig. 4. In the lower row, the figures are represented in the form of a density plot.

equivalent to magnon absorption by an up-spin electron. However, in the ferromagnetic saturation the system does not contain any magnon. That is the reason why at $T=0$ K the $\uparrow$ spectrum is without a scattering part. At finite temperatures ($\langle S^z\rangle/S=0.6$ in Fig. 4) the up-spin electron can absorb a magnon, therewith reversing its spin and subsequently forming a polaron. A weak polaron peak is therefore observable in Fig. 4 in the $\uparrow$ spectrum for the case of $\langle S^z\rangle/S=0.6$. The low energy peak in the $\downarrow$ spectrum is built up at finite temperatures, in principle, by two elementary processes. Because of finite deviations of the f spins from saturation the excited $\downarrow$ electron has a finite probability of entering the local frame of the f-spins as up-spin electron. This probability is zero for $\langle S^z\rangle=S$. On the other hand, it can first emit a magnon and by that reverse its spin becoming then an up-spin electron in the external frame of coordinates. Afterwards it enters with a certain probability the local frame as up-spin electron. In the second elementary process a magnon is involved, in the first it is not. The corresponding excitation energies differ more or less by a magnon energy which is however neglected in our treatment. The splitting of the spectral density into a polaron part and a scattering part is not restricted to the ferromagnetic phase, but remains for $T>T_c$ ($\langle S^z\rangle=0$), too. It represents a striking correlation effect that is by no means reproduceable in a one-electron picture. A respective angle and spin-resolved inverse photoemission experiment would require a careful interpretation since the excited single $(\mathbf{k},\sigma)$ electron produces two peaks in the spectrum with strongly wave-vector, spin, and temperature dependent spectral weights.

The splitting of the spectral density transfers itself to the quasiparticle density of states as a gap. This of course depends on the actual coupling strength J/W. For $J/W=0.2$, as in Fig. 5, the QDOS splits for both spin directions into two quasiparticle subbands, the position of which do not change very much with temperature. Only the gap becomes slightly wider with increasing temperature. The ordered magnetic state of the f system induces into the conduction band a remarkable spin asymmetry. This asymmetry gradually disappears with decreasing f magnetization $\langle S^z\rangle$; however, not by a Stoner-like shift of respective spin bands, but rather by a temperature-dependent shift of weight between the subbands. That means that the first-order term (48) of the electronic self-energy, which is proportional to $\langle S^z\rangle$, is overcompensated by the higher-order terms. The above mentioned redshift of the optical absorption edge is in such a case due to a quasiparticle band narrowing effect and not so much to a respective shift of the whole subband. For weaker couplings J/W the situation is changing drastically. The two subbands melt together shifting as a whole Stoner-like, i.e., proportional to $\langle S^z\rangle$, with increasing temperature. Then the mean-field part (48) of the self-energy dominates the spectrum. The ferromagnetic saturation ($\langle S^z\rangle=S$) in Fig. 5 represents the already mentioned special case for that the upper quasiparticle subband disappears in the $\uparrow$ spectrum.

To demonstrate the quasiparticle character of the various structures in the spectral density, we have plotted in Fig. 6 for three typical examples the contributions of the respective peak to the time-dependent propagator,

$$S_{\mathbf{k}\sigma}(t)=\frac{1}{2\pi\hbar}\int dE\; S_{\mathbf{k}\sigma}(E)e^{-(i/\hbar)Et}. \tag{77}$$

Since the peaks are rather sharp we could restrict the energy region for the Fourier transformation in (77) closely around the respective peak position. The polaron part of

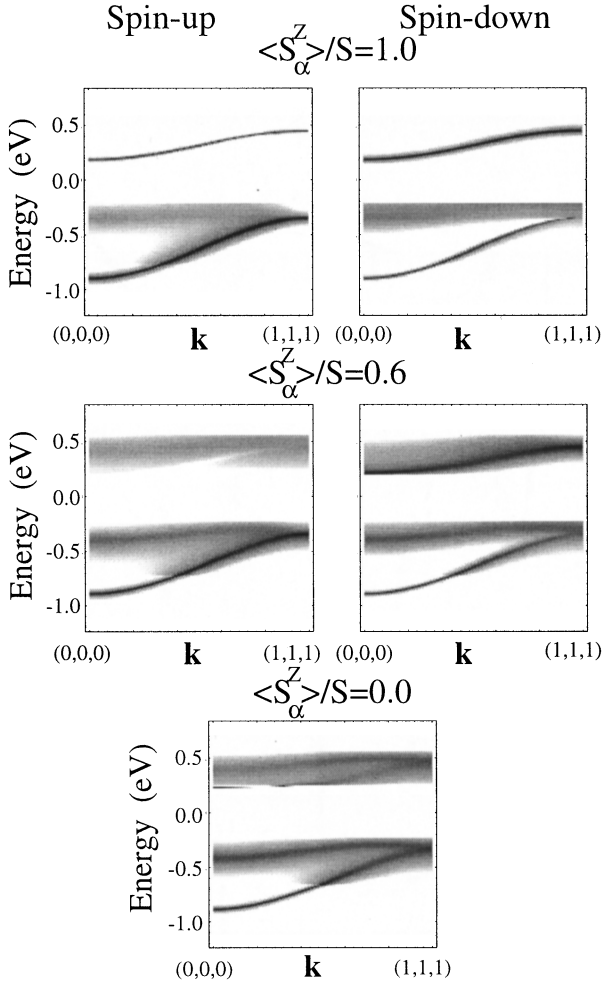

FIG. 8. Density plot of the sublattice spectral density of the antiferromagnetic semiconductor as function of energy for wave vectors from the (111) direction of the fcc-magnetic Brillouin zone. Results are plotted for three different sublattice magnetizations (parameters: $J=0.2$ eV, $S=7/2$; total lattice: sc; sublattice: fcc).

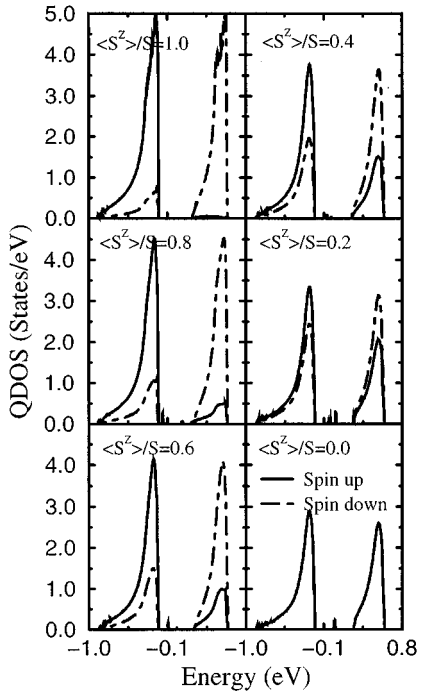

FIG. 9. Sublattice quasiparticle density of states $\rho_{A\sigma}(E)$ of the conduction band of the antiferromagnetic semiconductor as function of energy for various values of the *f*-spin sublattice magnetization. Full line for $\sigma=\uparrow$ and broken line for $\sigma=\downarrow$. Parameters as in Fig. 8. Symmetry: $\rho_{A\sigma}(E)=\rho_{B-\sigma}(E)$.

$S_{\mathbf{k}\downarrow}(E)$ at $\langle S^z\rangle=S$ is a δ function, so that $S_{\mathbf{k}\downarrow}(t)$ becomes an undamped oscillation, not plotted in Fig. 6. The corresponding scattering part leads for **k** vectors close to the Γ point to a damped oscillation. The lifetime of the oscillation turns out to be drastically **k** dependent (upper part in Fig. 6). This holds also for the two propagators at $T=T_c$. The propagator, which arises from the low energy peak in the spectral density, represents a rather long living quasiparticle (middle part of Fig. 6), at least for those **k** vectors chosen in the figure. The propagator from the upper peak of the $T=T_c$ spectral density exhibits a distinct wave-vector dependence of the quasiparticle lifetime (lower part of Fig. 6).

The J dependence of the exact $T=0$ down-spin spectral density, exhibited in Fig. 7, demonstrates the qualitatively different features for the weakly and strongly coupled *s-f* system. For small J only one quasiparticle dispersion appears, the system is describable in a single particle concept. For strong J the splitting into a polaron and a scattering peak takes place. In the intermediate region ($J=0.05$–0.1) the situation becomes fairly complicated. For some **k** vectors the splitting is clearly observable, for others not. In the strong coupling regime ($J\geqslant 0.15$ eV) the polaron peak consists of a δ function, representing a quasiparticle with infinite lifetime. Since the curves in Fig. 7 are exact results, they prove that the correlation caused splitting of the spectral density into a polaronic and a scattering portion is not at all an artefact of any unavoidable approximation used in the calculation. It is a fundamental feature of the underlying exchange-coupled physical system.

B. Antiferromagnet

As described in Sec. IV, we have evaluated our theory also for a two-sublattice antiferromagnet. The chemical lattice is simple cubic and the magnetic sublattice is face centered cubic. Figures 8–10 show the results for the sublattice spectral density and the quasiparticle density of states. The wave vector and spin-resolved excitation spectrum as it comes out from the sublattice spectral density has the obvious symmetry $(A,\sigma)\leftrightarrow(B,-\sigma)$. In that sense the spectral density $S^{\alpha\alpha}_{\mathbf{k}\sigma}(E)$ for sublattice α exhibits a spin asymmetry below the Neel temperature T_N. It is important to remember that **k** is a vector from the sublattice Brillouin zone. A majority-spin electron in sublattice A becomes a minority-spin electron in sublattice B and vice versa. The hopping between the sublattices therefore produces an excitation spectrum (Fig. 8) that is more complicated than that of the ferromagnet (Fig. 4). Each of the two quasiparticle structures in Fig. 4 is, in general, split once more because of the reduced magnetic Brillouin zone (''Slater splitting''). However, the detailed interpretation of the elementary process, which causes the spectral density structures, is exactly the same as in the ferromagnetic case. The sublattice quasiparti-

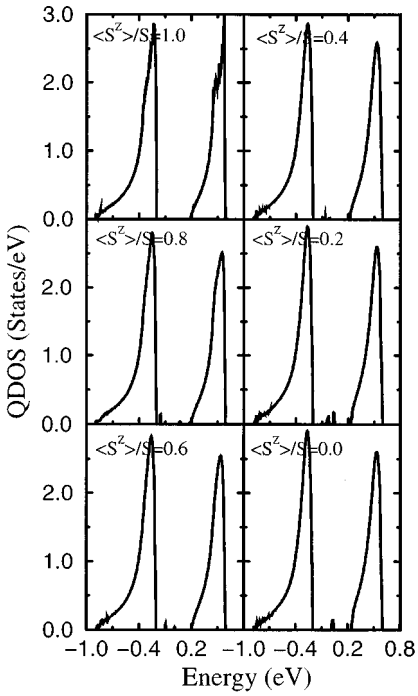

FIG. 10. Total quasiparticle density of states $\rho(E)$ of the antiferromagnetic semiconductor as function of energy for various values of the sublattice magnetization. Parameters as in Fig. 8.

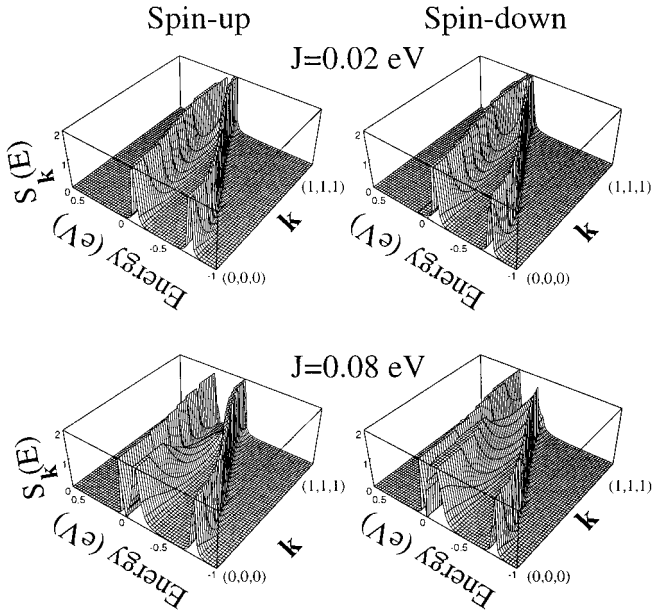

FIG. 11. Sublattice spectral density of the antiferromagnetic semiconductor at $T=0$ K as a function of energy for wave vectors from the (111) direction of the fcc-magnetic Brillouin zone. Results are plotted for two different exchange couplings. Parameters as in Fig. 8.

cle density of states $\rho_{\alpha\sigma}(E)$ (72) results from the spectral density by a wave-vector summation over the first Brillouin zone (Fig. 9). As for the ferromagnetic system (Fig. 5) it is composed for each spin direction of two quasiparticle subbands. Majority- and minority-spin spectra occupy exactly the same energy regions. That is of course a consequence of the intersublattice hopping by which the electron changes its character from a majority-spin to a minority-spin electron and vice versa. That is the reason why, contrary to the ferromagnet (Fig. 5), there appears even for $\langle S_\alpha^z\rangle = S$ a finite up-spin contribution in the upper part of the energy spectrum. We note in passing that our parameter choice $\langle S_\alpha^z\rangle = S$ is of course somewhat unrealistic since the localized spin system, also, cannot reach the full sublattice magnetization. That is a typical property of any antiferromagnet. The zero point deviation is, however, rather small. But even under the assumption that the spin system is in the so-called Neel state (full polarization of the spin sublattice), the conduction band quasiparticle states behave differently than those of the ferromagnet. The majority-spin electron is never in an eigenstate like (76).

A photoemission experiment cannot distinguish between the two sublattices (72). The sublattice QDOS is therefore not observable, but the total QDOS which is plotted in Fig. 10 for various temperatures, say various f-spin sublattice magnetizations is observable. The QDOS does not show a remarkable temperature dependence because the temperature variations of the two sublattices are more or less compensating each other.

The formation of separated polaron and scattering parts in the sublattice spectral density with increasing strength of the s-f exchange coupling (Fig. 11) appears much more complicated than in the ferromagnetic case (Fig. 7). The reason is of course the additional Slater splitting of each quasiparticle band. For not too weak s-f coupling, we have to again conclude that a respective inverse photoemission experiment cannot at all be understood within a one particle theory. The exchange coupling leads to drastic and unconventional correlation effects, so that the presentation of the spectrum in the usual way by a conventional (quasiparticle) band structure becomes rather doubtful.

VI. CONCLUSIONS

We have presented a theory for the energy spectrum of a single electron in an otherwise empty conduction band, which is coupled by an intra-atomic exchange interaction to a ferromagnetically or antiferromagnetically ordered localized-spin system. This situation is realized in ferromagnetic (antiferromagnetic) semiconductors like EuO (EuTe). Our approach uses a moment-conserving decoupling procedure for suitably defined Green functions. It turns out to be exact for the rigorously treatable, but nevertheless nontrivial limiting case of a single-electron exchange coupled to a ferromagnetically saturated f-spin system. Futhermore, it fulfills the exact zero-bandwidth limit.[24] The fact that our theory evolves continuously from the exactly solvable limiting cases to arbitrary temperature, finite bandwidths, and different magnetic spin structures gives it a certain trustworthiness.

The exchange coupling of the conduction electron to the spin system gives rise to some extraordinary correlation effects. In a ferromagnetic semiconductor the excitation spectrum is split into a polaronic and a scattering part. The polaron part may be interpreted as a repeated emission and reabsorption of a magnon by the conduction electron result-

ing in an effective attraction. The rather broad scattering part is due to a magnon emission or absorption by the conduction electron. It occupies the same energy region as the quasiparticle density of states of the opposite spin because emission or absorption of a magnon means a spin flip of the conduction electron. However, in most cases the scattering spectrum is bunched to a prominent quasiparticle peak. If J is smaller than a certain critical coupling, then the exchange interaction only leads to a renormalization of the one-electron energy. For higher values of J, the mentioned splitting into a polaronic and a scattering part happens; a fact that requires a rather unconventional interpretation of the respective inverse photoemission experiment. The usual $E=E(\mathbf{k})$ band structure representation becomes insufficient. A decisive quantity is, for instance, the spectral weight of the quasiparticle excitation, which regulates the relative importance of the various poles, i.e., the intensities of the corresponding photoemission line shapes. Because of the additional Slater splitting, the spectral density structure becomes still a bit more complicated for an antiferromagnetic semiconductor. Each quasiparticle dispersion splits once more due to the reduced magnetic Brillouin zone.

We intended to apply the presented model study to real substances such as EuO and EuTe. A first attempt for the ferromagnetic system EuO has already been performed,[25] however, based on a simpler theory. The quasiparticle band structure of the prototypical antiferromagnetic semiconductor EuTe is the next goal of our research work. We have to combine the presented many body theory with realistic one-electron band structure calculations performed within the framework of the density functional theory. The extension of the theory to antiferromagnetic metals[21] will allow us to investigate the highly interesting alloy $Yb_xGd_{1-x}Te$ that changes its physical behavior from a paramagnetic insulator (YbTe) via a spin glass phase to an antiferromagnetic metal (GdTe).[26] The corresponding magnetic phase diagram means a further challenge of our investigation.

ACKNOWLEDGMENT

This work has been sponsored by the ''Deutsche Forschungsgemeinschaft'' under the sign AFM/EuTe.

[1] E.L. Nagaev, Phys. Status Solidi B **65**, 11 (1974).
[2] W. Nolting, Phys. Status Solidi B **96**, 11 (1979).
[3] S.G. Ovchinnikov, Phase Transitions **36**, 15 (1991).
[4] P. Wachter, *Handbook of the Physics and Chemistry of Rare Earths*, edited by K.A. Gschneidner and L. Eyring (North Holland, Amsterdam, 1979), Vol. 1, Chap. 19.
[5] C. Haas, CRC Crit. Rev. Solid State Sci. **1**, 47 (1970).
[6] S. Legvold, *Ferromagnetic Materials*, edited by E.P. Wohlfarth (North Holland, Amsterdam, 1980), Vol. 1, Chap. 3.
[7] V. Eyert and W. Nolting, Solid State Commun. **60**, 905 (1986).
[8] J.R. Schrieffer and P.A. Wolf, Phys. Rev. **149**, 491 (1966).
[9] Y.A. Dimashko and A.L. Alistratov, Phys. Rev. B **50**, 1162 (1994).
[10] V.J. Emery, Phys. Rev. Lett. **58**, 2794 (1987).
[11] S.S.P. Parkin, N. More, and K.P. Roche, Phys. Rev. Lett. **64**, 2304 (1990).
[12] J. Unguris, R.J. Celotta, and D.T. Pierce, Phys. Rev. Lett. **67**, 140 (1991).
[13] D.M. Edwards, J. Mathon, R.B. Muniz, and M.S. Phan, Phys. Rev. Lett. **67**, 493 (1991).
[14] F. Shi, M. Ding, and T. Liu, Solid State Commun. **97**, 225 (1996).
[15] B.S. Shastry and D.C. Mattis, Phys. Rev. B **24**, 5340 (1981).
[16] S.R. Allan and D.M. Edwards, J. Phys. C **15**, 2151 (1982).
[17] W. Nolting and U. Dubil, Phys. Status Solidi B **130**, 561 (1985).
[18] S. Doniach, Physica **91B**, 231 (1977).
[19] C. Lacroix and M. Cyrot, Phys. Rev. B **20**, 1969 (1979).
[20] A.L. Fetter and J.D. Walecka, *Quantum Theory of Many Particle Systems* (McGraw-Hill, New York, 1971).
[21] W. Nolting, S. Rex, and S. Mathi Jaya (unpublished).
[22] H.B. Callen, Phys. Rev. **130**, 890 (1963).
[23] S. Bei der Kellen, W. Nolting, and G. Borstel, Phys. Rev. B **42**, 447 (1990).
[24] W. Nolting and M. Matlak, Phys. Status Solidi B **123**, 155 (1984).
[25] W. Nolting, W. Borgiel, and G. Borstel, Phys. Rev. B **37**, 7663 (1988).
[26] D. Ravot, A. Mauger, and O. Gorochov, Phys. Rev. B **48**, 10 701 (1993).